U.P.B. Sci. Bull., Series D, Vol. 73, Iss. 4, 2011 ISSN 1454-2358

INDENTATION TESTS TO STUDY THE MECHANICAL TRIBOLOGICAL PROPERTIES OF UHMWPE

Georgiana CHIŞIU[1], Tiberiu LAURIAN[2], Andrei TUDOR[3]

Scopul acestui studiu este de a analiza procesul de indentare cu frecare a unei suprafeţe plane din UHMWPE, de către unui indentor conic rotunjit la vârf. O serie de indentări au fost făcute pe două tipuri de polietilenă una conveţională şi cealaltă iradiată cu raze γ, folosite în cuplele de frecare din articulaţiile artificiale de şold. Răspunsul la indentare a polimerilor depinde în principal de structura chimică a acestora şi de o serie de parametri cum ar fi viteza de indentare, forma, mărimea, natura indentorului şi starea de lubrifiere. Se propune un model de comportare Zener modificat la indentare a polietilenei. Experimentările realizate confirmă calitativ rezultatele analitice pentru modelul Zener modificat propus.

The goal of this study was to examine the penetration energy loss by the normal rigid conical indenter into Ultra High Molecular Weight Polyethylene (UHMWPE) surfaces. A series of indentation tests were carried out on two types of UHMWPE: non-irradiated (conventional) and gamma irradiated (crosslinked). Indentation response of polymers depends mainly on the nature of the polymer and the operating parameters such as indentation velocity and shape, size and nature of the indenter and lubrication conditions. In our study we have used the microindentation technique to study the behaviour of two types of UHMWPE. We considered the viscoelastic Zener material modified model. Experiments carried out confirm the quality of analytical results for the modified Zener model proposed.

Keyword: indentation, UHMWPE, friction, polymer rheology

Nomenclature

a	contact radius
A	contact aria
a_a	dimensionless contact radius (a/R)
a_s	limit contact radius
F_{aS}	dimensionless Stribeck contact pressure ($F_n/(\pi R^2 G_2)$)
F_n	indentation load
F_d	friction force caused by inner material interactions

[1] Assistant professor, Dept. of Machine design and Tribologie, University POLITEHNICA of Bucharest, Romania, e-mail: georgiana_bosoi@yahoo.com
[2] Lector, Dept. of Machine design and Tribologie, University POLITEHNICA of Bucharest, Romania, e-mail: tlaurian@gmail.com
[3] Professor, Dept. of Machine design and Tribologie, University POLITEHNICA of Bucharest, Romania, e-mail: tudor@meca.omtr.pub.ro

g_{12}	elasticity ratio (G_1/G_2)
G1, G2	transversal modulus of elasticity
m_e	strain rate sensivity of viscoelastic solids
p	contact pressure
R	spherical tip radius
t	time
t_a	dimensionless time (t/t_i)
t_i	creep time (η_e/G_2)
t_{oa}	dimensionless time to peak load
t_{oSc}	dimensionless residual time
v	penetration velocity
v_a	dimensionless penetration velocity ($\eta_e v/(G_2 R)$)
α	half con angle
γ	hysteresis lost coefficient
δ	penetration depth
δ_p	plastically deformed depth
$\dot{\delta}$	strain rate penetration
δ_a	dimensionless penetration depth (δ/R)
δs	limit penetration depth
η_e	equivalent dynamic viscosity
η_2	apparent dynamic viscosity
μ	friction coefficient
τ_f	shear stress
Φ_m	creep function
Φ_{am}	dimensionless creep function ($\Phi_m G_2$)
Ψ_m	relaxation function
Ψ_{am}	dimensionless relaxation function (Ψ_m /G_2)
Index	
i, d	loading, unloading

1. Introduction

Ultra High Molecular Weight Polyethylene (UHMWPE) a member of the semi-crystalline polymer family is very resistant to abrasion, being used as the polymer of choice in modern hip and knee replacement components [1].

For the last five decades, orthopaedic surgeons have successfully used UHMWPE, taking advantage of its toughness, durability and biological inertness, as bearing surfaces in total joint replacements components against both metallic and ceramic surfaces [2].

The average lifetime of a total hip or knee replacement is considered to be between 15 and 20 years, leaving great hope for recovery for those benefiting from over 700,000 such procedures conducted successful in 2004 in USA [3].

Projections show that the overall number of total joint replacements will greatly increase by 2030, reaching 850,000 to 4.3 million hip and knee replacement procedures [4]. The same report stated that the reasons for revisions of primary total knees were aseptic loosening (33%), followed by UHMWPE wear (30%) and instability (17%) [3].

The main factor that might or can prevent total joint arthoplasties from achieving a lifetime of usage is the possibility of mechanical failure of the UHMWPE components. Studies have shown that mechanical failures that happen in vivo are usually due to wear or fatigue, actions that induce damage and are caused by the sliding motion between metallic and UHMWPE components [5].

Because of the need to increase the long-term performance of total joint arthroplasties, many researchers have conducted extended studies on the phenomena involved in the mechanism behind the UHMWPE surface damage.

Although such efforts have been made in the search for proper methods of controlling the damage exerted on the surface of UHMWPE components, the micro-mechanics involved in such processes are not yet fully understood. It must be noted that UHMWPE is a mix between amorphous and semi-crystalline states.

Up-till recently the models that have been used to describe the effects on UHMWPE have been constructed in a large percentage out of metal based materials that employed the use of a flow rule [6], [7]. The impingement phenomena of femoral head to acetabular polyethylene cup were observed in the revision hip prosthesis.

This type of modelling is not adequate for UHMWPE due to the fundamental differences in the deformation mechanisms of polymers and metals. In amorphous polymeric materials orientation strain hardening due to polymer chain stretching and alignment in the amorphous regions is a primary deformation mechanism [7]. These constitutive relations are a model for both viscoelastic and viscoplastic behaviours.

We adopted an evolving state model where the state variables are considered to evolve with the deformation according to a rate-equation. The energy loss in the damage process of polyethylene can be used as an indicator of the friction and wear phenomena.

The goal of this study was to examine the indentation phenomena and the penetration energy loss by the normal rigid conical indenter in the UHMWPE. A series of indentation tests were carried out on two types of UHMWPE: non-irradiated (conventional) and gamma irradiated (crosslinked). The indentation is defined as a mechanical deformation process where a controlled force or displacement is exerted on a hard tip to indent onto a surface up to a certain depth and then retract from the surface.

2. Rheologic and tribological model

UHMWPE exhibits a time-dependent stress-strain relationship which is described as viscoelastic in the first part of total stress-strain curve. The common feature of viscoelastic behaviour is the variation of strain in a specimen of material under the action of a constant stress applied for a time period. The strain shows an initial elastic response to the applied stress and a delayed elastic strain. This material behaviour can not be incorporated into a rigorous theory of contact provided that the viscoelastic stress-strain relationship of the material can be considered to be nonlinear [8].

Thus, for linearity, an increase in the stress by a constant factor must produce an increase in the strain response by the same factor [8].

The stress-strain relation for a linear viscoelastic material can be expressed in the creep compliance function. This function gives the strain response to a step change in stress or, alternatively, in the relaxation function which expresses the stress response to a step change in strain.

We adopted viscoelastic behaviour of UHMWPE according to the modified Zener model Fig. 1. This model is characterized by two springs of modulus of elasticity G1 and G2, together with a dashpot of viscosity η_2 and external friction of polyethylene (μ) with the penetrator. The effect of external friction can be used to consider an equivalent viscosity of polyethylene.

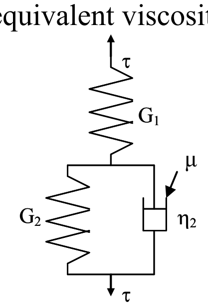

Fig. 1. Viscoelastic Zener material model.

It has been accepted, in this modified Zener model, that viscosity η_2 is an internal friction parameter of UHMWPE. From the experimental data obtained in this work one can observe that the behaviour of UHMWPE indentation tests depends of velocities of the indenter and the condition of tests, if the contact of indenter with surface of UHMWPE is dry or wet.

Thus, it is necessary to modify the Zener model, by replacing the linear dashpot of viscosity η_2 with a nonlinear dashpot of viscosity η_e with external friction μ.

It is considered the power law of the fluid friction, $\tau_f = \eta_2 \dot{\varepsilon}_o (\dot{\delta} / \dot{\delta}_o)^{m_e}$, and Coulomb external friction, μp.

Thus, the force from dashpot is defined as $F_{nv} = A\tau_f + \mu F_n = A\eta_e \dot{\varepsilon}_o (v / v_o)^{m_e}$,

where $\dot{\varepsilon}_o \equiv 1/s$, $v_o = \dot{\delta}_o = 1\, mm/s$ are constants introduced for dimensional consistency.

We adopted a global friction parameter of UHMWPE (internal and external) named equivalent viscosity (η_e):

$$\eta_e = \eta_2 + \frac{\mu F_n}{(v / v_o)^{m_e} \dot{\varepsilon}_o} \tag{1}$$

This global friction parameter can be evaluated by experimental indentation data.

We applied the procedure described in [8], to analyse the effect of viscoelasticity on the contact pressure and strain for the spherical contact between the flat UHMWPE surface and indenter's spherical - tip.

The dimensionless creep (Φ_{am}) and relaxation (Ψ_{am}) of a viscoelastic material are described by the following relations, as a condition to connect the Zener deformation with the normal load:

$$\Phi_{am} = \Phi_m \cdot G_2 = \frac{1}{g_{12}} + \left(1 - \exp\left(-t_a\right)\right) \tag{2a}$$

$$\Psi_{am} = \frac{\Psi_m}{G_2} = \frac{g_{12}}{1 + g_{12}} \cdot \left[1 + g_{12} \cdot \exp(-t_a \cdot (1 + g_{12}))\right] \tag{2b}$$

The dimensionless creep and relaxation responses of a modified Zener material, Φ_{am} and Ψ_{am} are shown in Fig. 2, as functions of the dimensionless time t_a for several values of the elasticity ratio g_{12}. The elasticity ratio (g_{12}) for UHMWPE can be used with some technical reserve. Thus, the elasticity moduli of crosslinked UHMWPE at 110^{o}C are approximated with G_1 = 655 MPa and G_2 =82 MPa. These values are evaluated by the uniaxial tension and compression curves obtained experimentally at room temperature by Bergstrom [6], [7] and the Poisson coefficient ν = 0.46. Other authors obtained similar shape experimental curves for uniaxial tension, but different values for the elasticity moduli [5], [9].

In the proposed theoretical model, it is considered the elasticity ratio (g_{12}) and the equivalent viscosity (η_e) to be the most important parameters. The equivalent viscosity is analysed thus as variable.

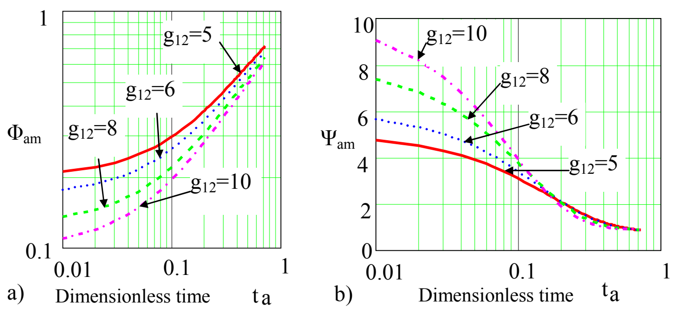

Fig. 2. Creep and relaxation function of a modified viscoelastic Zener material model.

We shall examine the material response when a rigid cone with a spherical tip is pressed against a viscoelastic solid. Under the action of a constant indentation force, the penetration of the indenter and the contact area will both grow and the distribution of contact pressure will change. The variation of contact area and pressure distribution is analyzed for any prescribed variation of loading or penetration. We adopted the suggestion of Radok, mentioned by Johnson [8], for finding the stresses and deformations in cases where the corresponding solution for a purely elastic material is known.

Thus, it consists of replacing the elastic constant in the elastic solution by the corresponding integral operator from the viscoelastic stress-strain relations. If the deformation history is known, the stresses are found by replacing elasticity modulus, 2G, in the elastic solution by the integral operator, expressed in terms of the relaxation function. If the load or stress history is known, the variation in deformation is found from the elastic solution by replacing the constant 1/2G with the integral operator involving the creep compliance $\Phi_m(t)$.

We analysed the contact of rigid conical-spherical penetrator with the viscoelastic surface. The geometry of this penetrator is shown in the Fig. 3. In order to obtain a generalisation of the analytical model, both penetration depth and contact area radius were normalized δ_a, a_a.

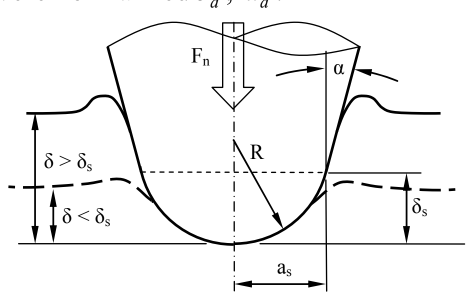

Fig. 3. Geometry details of the indentation.

When the contact corresponds to the limit of the spherical and conical regions Fig. 3, the critical dimensionless depth δ_{as} is defined as:

$$\delta_{as}(\alpha) = 1 - \sin\alpha \tag{3}$$

The dimensionless contact radius of the indenter can be written as:

$$a_a = \begin{vmatrix} \sqrt{2\cdot\delta_a - \delta_a^2}, & if\ \ 0 \le \delta_a \le \delta_{as} \\ \left(\delta_a + \dfrac{1-\sin\alpha}{\sin\alpha}\right)\cdot\tan\alpha, & if\ \ \delta_{as} < \delta_a \end{vmatrix} \tag{4}$$

When the indentation velocity v is known, the dimensionless depth can be calculated as:

$$\delta_a = \begin{vmatrix} v_a \cdot t_a, & if\ \ 0 \le t_a \le t_{oa} \\ v_a \cdot t_{oa} \cdot \left(2 - \dfrac{t_a}{t_{oa}}\right), & if\ \ t_{oa} < t_a \le 2t_{oa} \end{vmatrix}, \tag{5}$$

where the dimensionless velocity is defined as $v_a = \dfrac{\eta_e \cdot v}{G_2 \cdot R}$.

This contact radius has a variation in time as illustrated in Fig.4. The relative dimensionless contact radius (a_{ats}) is defined as a ratio of the contact radius at time t_a and the initial contact radius (the radius at time $t_a = 0$).

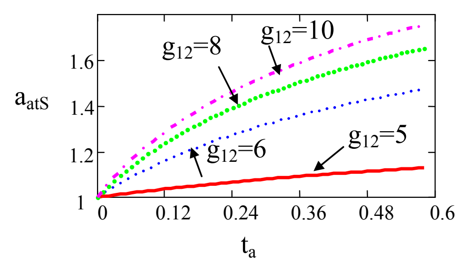

Fig. 4. The dimensionless contact radius of the indenter with dimensionless time.

When a conical indenter with spherical tip is pressed against a viscoelastic solid, the dimensionless radius of the contact circle a_a and the dimensionless penetration δ_a are linked by equation (6), which defines the creep response (s) to a step charge:

$$s(t_a) = \int_0^{t_a} \psi(t_a - x)\cdot\frac{da_a^3}{d\delta_a}dx \tag{6}$$

The dimensionless Stribeck contact pressure is numerically evaluated as a function of normal load and projected contact area. The dimensionless Stribeck contact pressure for the contact between sphere with radius R and a plane, under normal load F_n is $F_{aS} = F_n/(\pi R^2 G_2)$.

If the dimensionless penetration $\delta_a(t)$ has a prescribed variation, then, the dimensionless contact radius $a_a(t)$ varies according to the following equation:

$$a_a(t) = \sqrt{\delta_a(t)}, \tag{7}$$

This can be substituted in equation (5) to find the dimensionless Stribeck contact pressure:

$$F_{aSi}(t_a) = \frac{8}{3\pi} \cdot \int_0^{t_a} \psi(t_a - x) \cdot \frac{d}{dx} a_a^3(t_{oa})\, dx, \tag{8a}$$

$$F_{aSd}(t_a) = \left| \begin{array}{l} 0,\ if\ 0 \le t_a \le 1 - t_{as} \\ F_{aSi}(1 - 1t_a),\ if\ 1 - t_{as} < t_a \le t_{oa} \end{array} \right., \tag{8b}$$

$$F_{aSci}(t_a, \alpha) = \frac{8}{3\pi} \cdot \int_0^{t_a} \psi(t_a - x) \cdot \frac{d}{dx} a_a^3(t_{oa}, \alpha)\, dx, \tag{9}$$

$$F_{aScd}(t_a, \alpha) = \left| \begin{array}{l} 0, \quad if\ 0 \le t_a \le 1 - t_{ast} \\ F_{aSci}(1 - t_a, \alpha),\ if\ 1 - t_{as} < t_a \le t_{oa} \end{array} \right., \tag{10}$$

where F_{aSci} is loading force and F_{aScd} is unloading force when the contact of the tip corresponds to the conical region.

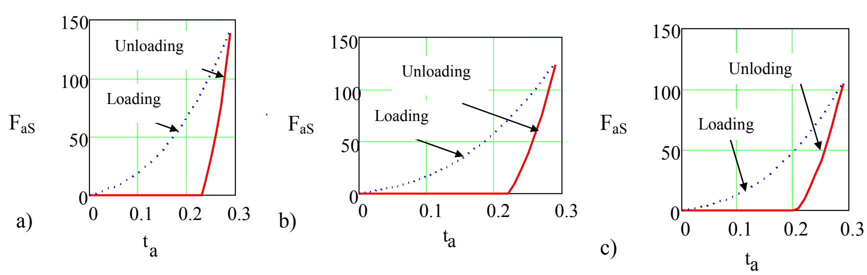

Fig. 5. Dimensionless Stribeck contact pressure - for cone with $\alpha = 30^0$. $g_{12} = 10$; b) $g_{12} = 8$; c) $g_{12} = 6$.

For example, Fig. 5 a), b) and c) shows the dimensionless Stribeck contact pressure for spherical and conical tip. These analytical curves were obtained for the following parameters: $g_{12} = 10$, $g_{12} = 8$, $g_{12} = 6$ $v_a = 2.46$ and $t_{oa} = 6.48$.

The lost energy by indentation with a spherical tip is given by the area of loading and unloading curves in time:

$$L_{ms} = \int_0^{t_{oa}} F_{aSi}\, dt_a - \int_{t_{oa}}^{t_{os}} F_{aSd}\, dt_a, \tag{11}$$

where t_{os} is dimensionless time corresponding to unloading Stribeck pressure decreases to zero $F_{aSd} = 0$ (as shown in Fig. 6 a). This time can be evaluated by numerically.

The lost energy by indentation when the contact has been in the conical region can be evaluated similarly to a spherical tip:

$$L_{mcs} = \int_0^{t_{oa}} F_{aSci}\, dt_a - \int_{t_{oa}}^{t_{osc}} F_{aScd}\, dt_a , \qquad (12)$$

where t_{osc} is dimensionless time corresponding to unloading Stribeck pressure decreases to zero $F_{aScd} = 0$ (as shown in Fig. 6 a).

The hysteresis lost coefficient energy is defined that report of the lost energy and the loading energy as shown Fig. 6 a). This hysteresis lost coefficient can be used that first parameter to obtainer the wear particle of UHMWPE.

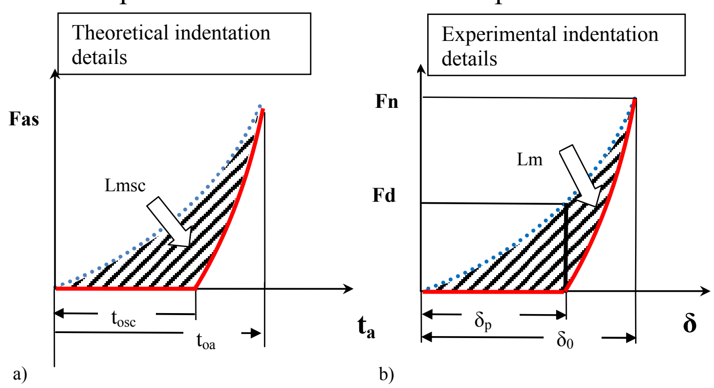

Fig. 6. Indentation force and energy lost during an indentation (Lm) calculated with analytical method (a) and determined experimentally (b).

Thus, the hysteresis lost coefficient has form:

- for spherical tip, when $0 \le \delta_a \le \delta_{as}$:

$$\gamma_{ms} = \frac{L_{ms}}{\int_0^{t_{oa}} F_{aSi}\, dt_a}, \qquad (13)$$

- for conical contact region, when $\delta_{as} < \delta_a$:

$$\gamma_{mcs} = \frac{L_{mcs}}{\int_0^{t_{oa}} F_{aSci}\, dt_a}, \qquad (14)$$

3. Experimental details

Beside the analytical approach, the mechanical and tribological properties of the given samples were analyzed through micro-scale indentation tests. The indentation tests were performed with the UMT 2 tribometer (CETR, Campbell, CA, USA). This apparatus can accurately control and measure the applied loads, displacements and velocities of the indenter. The hard indenters used in these tests were diamonds of conical shape with tip angles of 60°. The tip radius of the indenter was measured to be 12.5 μm.

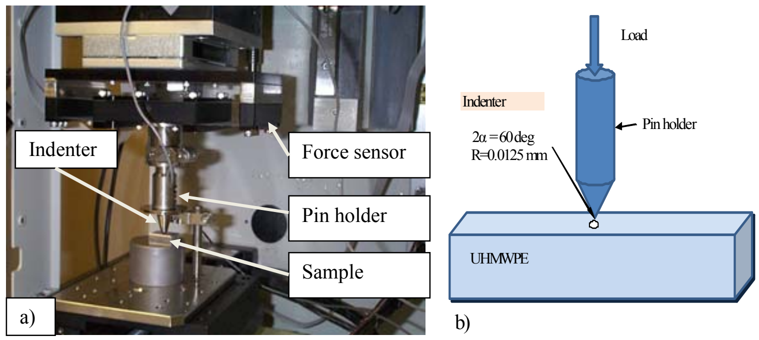

Fig. 7. Indentation test details.
a) UMT Micro-indentation test set-up; b) Schematic of indentation test set-up.

A series of indentation tests were carried out on two types of UHMWPE: non-irradiated (conventional) CPE and gamma irradiated (crosslinked) XPE and the mechanical properties of these materials are presented in *Table 1*.

Table 1

The mechanical properties of conventional UHMWPE and crosslinked [9], [11]

Property	**UHMWPE**	**XPE**
Irradiation	0 kGy	50kGy
Degree of Crystallinity [%]	53.6±6.2	45.3±5.3
Poisson's Ratio	0.46	0.46
Tensile Modulus of Elasticity (MPa)	915±423	860±206
Tensile Yield Strength (MPa)	25.6±3.3	21.1±2.5
Tensile Ultimate Strength (MPa)	231.1	157.7
Tensile Ultimate Elongation (%)	317±140	212±61

The conventional UHMWPE samples were cut from extruded sheets of UHMWPE GUR 1050 with surface area measuring 30mm × 80mm and thickness of 4mm. The cross-linked UHMWPE samples were cut from the acetabular component of a hip prosthesis with thickness of 4mm.

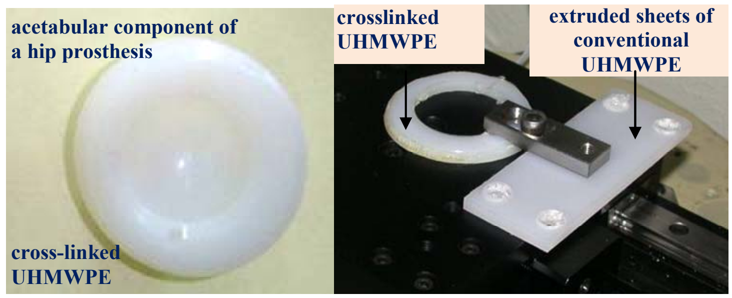

Fig. 8 The UHMWPE samples tested.

The maximum load was limited to 9N assuming that a 10 *N* (1 kg) force sensor is installed in UMT. The indentation velocities were 0.01 *mm/s*, 0.02 *mm/s*, 0.04 *mm/s* and *0.08 mm/s.* All tests were performed with indentation depths at 0.2 *mm* into the UHMWPE surface. Two test conditions where employed: dry and wet contact. These conditions were used in order to account for the effect of indenter lubrication. For wet contact tests were performed using a saline solution (0.9 % NaCl) in order to replicate the *in vivo* environment.

The test surfaces were ground with silicon carbide paper progressively with higher grades up to grade 1000. The mean roughness of the samples was 0.2± 0.03 μm. All the indentation tests were performed on 4 different specimens. The variability in the force between the repeated tests was less than 7% and the experimental results that are presented in our paper are the median force indentation depth curve for each condition.

4. Experimental results

Fig. 9 and Fig. 10 show the load-displacement curves for the viscoelastic material in contact with the conical indenter (hysteresis curve) under dry and wet conditions.

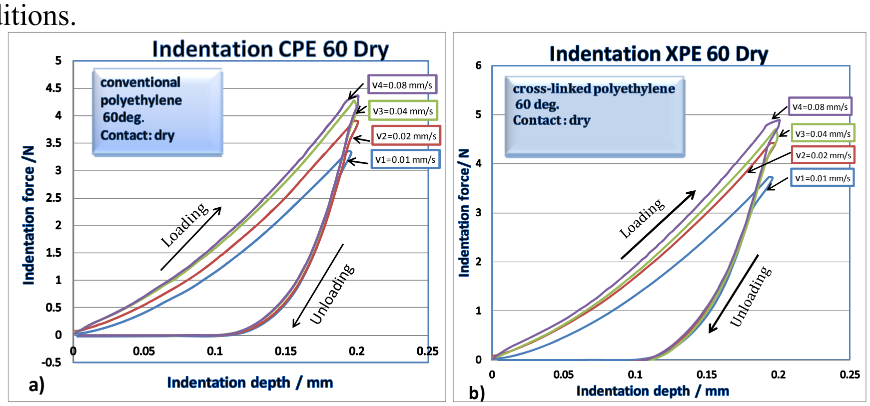

Fig. 9. Experimental load-displacement curves for conventional and cross-linked UHMWPE for dry contact.
a) Conventional UHMWPE; b) Cross-linked UHMWPE

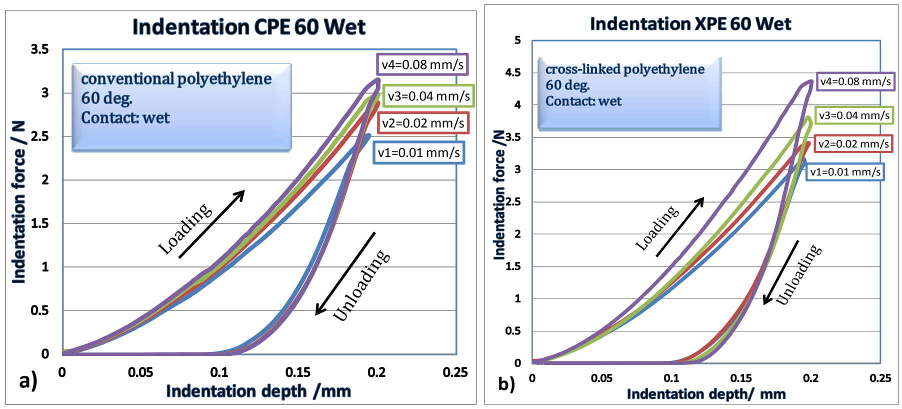

Fig. 10. Experimental load-displacement curves for conventional and cross-linked UHMWPE for wet contact.
a) Conventional UHMWPE; b) Cross-linked UHMWPE

The response of the surface to indentations for different velocities and lubrication condition is influenced by the mechanical properties of the material and it is observable in the Fig. 9 and Fig. 10. For an example, the peak indentation force of 4.895 N for cross-linked UHMWPE is higher than the peak indentation force of 4.367 N for conventional UHMWPE, both materials being tested in dry condition. The peak indentation force of 4.195 N for cross-linked UHMWPE is higher than the peak indentation force of 3.159 N for conventional UHMWPE, both materials being tested in wet condition.

The normal force increases with the indentation velocity according to a power law.

The indentation force for dry contact is always greater than for wet contact, regardless of material type.

Table 2

Experimental results

XPE 60 deg.	**Fn [N]**	**δ_0 [mm]**	**T [sec.]**	**v [mm/s]**	**δ_p [mm]**	**δ_0-δ_p [mm]**	**F_d [N]**
Dry	4.895	0.19	2.44	0.08	0.10	0.0922	1.722
Wet	4.298	0.1935	2.46	0.08	0.10	0.094	1.361
CPE 60 deg.	**Fn N**	**δ_0 mm**	**T sec.**	**v mm/s**	**δ_p mm**	**δ_0-δ_p mm**	**Fd N**
Dry	4.36	0.20	2.46	0.08	0.11	0.09	1.89
Wet	3.158	0.20	2.47	0.08	0.10	0.10	1.01

The loading-unloading force difference (see *Table 3*), Fd, is greater for XPE than for CPE and it may be a useful quantity to evaluate the rheologic properties for materials subjected to sliding contacts (see also Fig. 6 b). Fd is a friction parameter that can be used for polyethylene wear resistance assessment.

The experimental curves shown in figures 9 and 10 have identical shapes with theoretical curves shown in figures 5 a, b, c.

To generalize the results, it is necessary to develop a procedure to determine the equivalent viscosity and the strain rate sensitivity.

The significant difference between the loading and unloading curves allows for evaluation of the energy loss coefficient due to inner material friction (γ) and due to friction between the indenter and UHMWPE contact surface. This coefficient is presented in *Table 3*.

Table 3

The energy loss coefficient due to inner material friction

	CPE 60 deg.		**XPE 60 deg.**	
	Dry	**Wet**	**Dry**	**Wet**
Fn [N]	4.367	3.158	4.895	4.195
Fas	108.492	78.45	121.61	104.219
γ				
V_1=0.01[mm/s]	0.623	0.522	0.579	0.560
V2=0.02[mm/s]	0.628	0.555	0.595	0.550
V3=0.04[mm/s]	0.653	0.547	0.621	0.600
V4=0.08[mm/s]	0.641	0.562	0.612	0.582

The energy loss coefficient depends on indentation velocity and contact lubrication. It can be observed that energy loss is always lower for wet contact tests. In the case of XPE, the maximum energy loss occurs for velocity v_3 =0.04mm/s, rather than for v_4 =0.08mm/s. This situation may happen because the friction coefficient between the indenter and UHMWPE surface may decrease after a certain sliding velocity.

The energy loss coefficient is lower for XPE than for CPE. This observation confirms the superior tribological behaviour of XPE (lower friction coefficient and greater wear resistance).

This peak indentation force corresponds to dimensionless Stribek pressure and the value can be obtained by replacement in this expression $F_{aS} = F_n / (\pi R^2 G_2) = \dfrac{4.367}{\pi \cdot 0.0125^2 \cdot 85} = 108.492$.

The equivalent viscosity (η_e) and strain rate sensivity (m_e) were determined from experimental indentation data in the following way: knowing the indentation curves (loading-unloading) for two velocities, the maximum indentation depth (δ), plastically deformed depth (δ_p) and maximum load (F_n) can be recorded. Thus, the calculated equivalent viscosity and strain rate sensitivity for the dry condition of conventional UHMWPE is η_e = 31.62 MPa and m_e = 0.117.

5. Conclusions

A model for the contact between a conical indenter with spherical tip and an UHMWPE surface has been developed using the rheologic and tribological approach.

Also, an experimental study has been elaborated for the analysed problem. The instrumented indentation tests revealed that crosslinking of UHMWPE induces significant modifications about friction lost and loading capacity.

The hysteresis area depends on the indentation velocity and the viscosity effect of UHMWPE. The energy loss in the damage process of polyethylene can be used as an indicator of the wear phenomena.

The theoretical dimensionless Stribeck pressure has a similar aspect as the experimental data.

Indentation can be considered as a useful method for evaluating tribological and rheological properties of UHMWPE.

REFERENCES

[1] *S.K Sinha., W.L.M Chong., S.C Lim.*, Scratching of polymers – Modelling abrasive wear, Wear **vol. 262**, pp. 1038-1047, 2007.

[2] *S Kurtz*., The UHMWPE Handbook, Elsevier Academic press, 2004.

[3] *K Karuppiah., S Sundararajan*, *Xu ZHI, Li XD*, The effect of protein adsorption on the friction behavior of ultra-high molecular weight polyethylene, Tribology Letters **Vol. 22** no.2, pp.181-188, 2006.

[4] *S Kurtz., K Ong*, Projections of primary and revision hip and knee arthroplasties in the United States from 2005 to 2030, Journal of Bone and Joint Surgery **Vol. 89**, pp. 780-785, 2007.

[5] *M.C Sobieraj., C.M Rimnac*., Ultra high molecular weight polyethylene: Mechanics, morphology, and clinical behavior, Journal of the mechanical behavior of biomedical materials V**ol. 2**, pp. 433-443, 2009.

[6] *J Bergstrom., C.M Rimnac*, *S.M. Kurtz,* Prediction of multiaxial mechanical behavior for conventional and highly crosslinked UHMWPE using a hybrid constitutive model, Biomaterials **Vol. 24**, pp. 1365-1380, 2003.

[7] *J.S Bergstrom, S.M Kurtz*, *C.M Rimnac, A.A Edidin,* Constitutive modeling of ultra-high molecular weight polyethylene under large - deformation and cyclic loading conditions, Biomaterials **Vol. 23**, pp. 2329-2343, 2002.

[8] *K. L Johnson*, Contact mechanics, Cambridge University Press.; Cambridge, 1985.

[9] *K. S Simis., A. Bistolfi, A. Bellare, L. Pruitt*., The combined effects of crosslinking and high crystallinity on the microstructural and mechanical properties of ultra high molecular weight polyethylene, Biomaterials **Vol. 27**, pp. 1688-1694, 2006.

[10] *G. Kermouche, J.L. Loubet, J.M. Bergheau*, Extraction of stress-strain curves of elastic-viscoplastic solids using conical/pyramidal indentation testing with application to polymers, Mechanics of Materials **Vol**. **40**, pp. 271-283, 2008.

[11] *G. Lewis*, Properties of crosslinked ultra-high-molecular-weight polyethylene, biomaterials **Vol. 22**, pp. 371-401, 2001.